Cell Reports, Volume *33*

Supplemental Information

A Pushing Mechanism for Microtubule Aster Positioning in a Large Cell Type

Johnathan L. Meaders, Salvador N. de Matos, and David R. Burgess

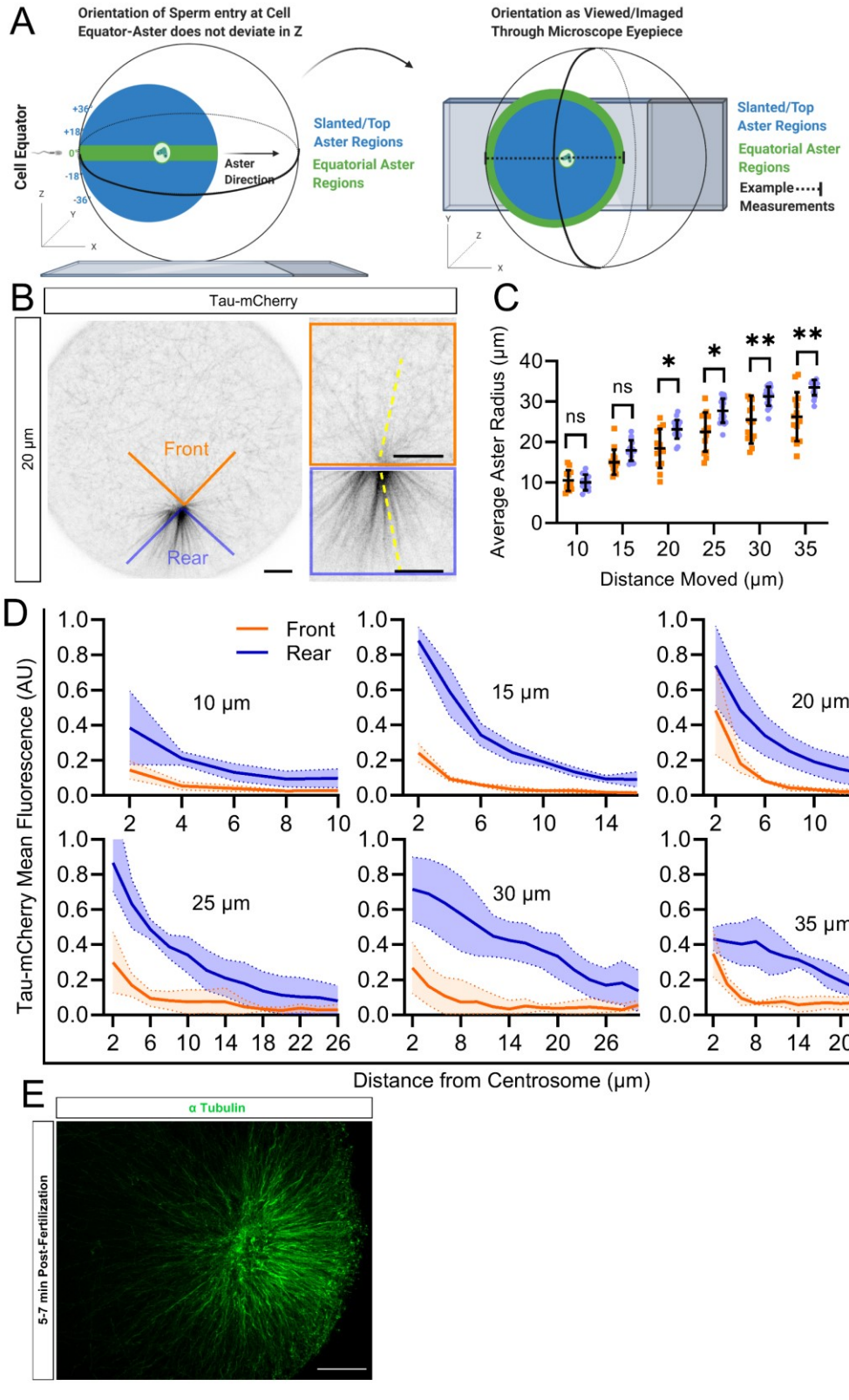
A
Orientation of Sperm entry at Cell Equator-Aster does not deviate in Z
Orientation as Viewed/Imaged Through Microscope Eyepiece
Cell Equator
Aster Direction
Slanted/Top Aster Regions
Equatorial Aster Regions
Example Measurements
B
Tau-mCherry
20 µm
Front
Rear
C
Average Aster Radius (µm)
Distance Moved (µm)
ns
*
**
D
Front
Rear
10 µm
15 µm
20 µm
25 µm
30 µm
35 µm
Tau-mCherry Mean Fluorescence (AU)
Distance from Centrosome (µm)
E
α Tubulin
5-7 min Post-Fertilization

Figure S1. Additional live-cell geometry and density quantification of asters, Related to Figure 1

(A) Sample orientation for live and immunofluorescence imaging and analysis. Cells were selected for imaging in which the sperm enters the egg +/- 10 μm from the egg equator along the Z-axis (Left cartoon). The sperm aster migrates along the cell equator, without deviating in Z, toward the cell center. By orienting the cell and sperm aster in this way, any slanted MTs in the Z-axis (Blue Regions) are defined as top and bottom portions of the sperm aster. Conversely, equatorial portions of the sperm aster (Green Regions) in front and behind the MTOC are defined as front and rear radii, respectively. Due to the spherical geometry of the aster, these front and rear equatorial radii represent the longest portions of the aster in the front and rear, respectively. We quantify the average maximum distance from the MTOC in front and rear equatorial portions using maximum intensity Z-projections of immunofluorescence images (Right Cartoon and Figure 1C-1D). This orientation allows us to exclude slanted top/bottom portions from our measurements because they do not reach the maximum radii of the sperm aster in front and rear equatorial portions (Right Cartoon, maximum boundaries are Green Equatorial Regions). In our live imaging, we use a single Z-plane through the MTOC of the sperm aster (Green Equatorial Region). The top and bottom portions of the sperm aster exit this Z-plane (Blue Regions), excluding them from our analysis (in reference to Figures 1A-1B and S1B-S1C).

(B) and (C) Tau-mCherry signal from zygotes imaged in Figure 1A and 1B. Tau-mCherry labeled MTs were measured from their most distal ends to the MTOC (yellow dashed line) in front (orange) and rear (blue) portions of the aster and averaged (Lfront and Lrear, respectively). Average Lfront and Lrear was calculated at time points in which the aster had moved 10, 15, 20, 25, 30, and 35 μm from the point of sperm entry (B). Data represent mean ± SD (n=16 zygotes), *P<.05, **P<.01, 2-way ANOVA with Sidak's multiple comparisons. See also Movie S1

(D) Densities of front and rear portions of the aster measured by Tau-mCherry mean fluorescence using the same ROI as in (A), as a function of distance from the centrosome. Fluorescence intensity is normalized to the MTOC for all data points (see materials and methods for more info.). Data represent the mean, shaded regions represent ± SD (n=9). P<.01

(E) Representative structured illumination microscopy image of the sperm aster ~10 minutes post-fertilization. Image represents a Z-stack of 50 μm 3D volume at 0.5 μm. intervals converted to a maximum intensity projection.

Scale bars, 10 μm throughout.

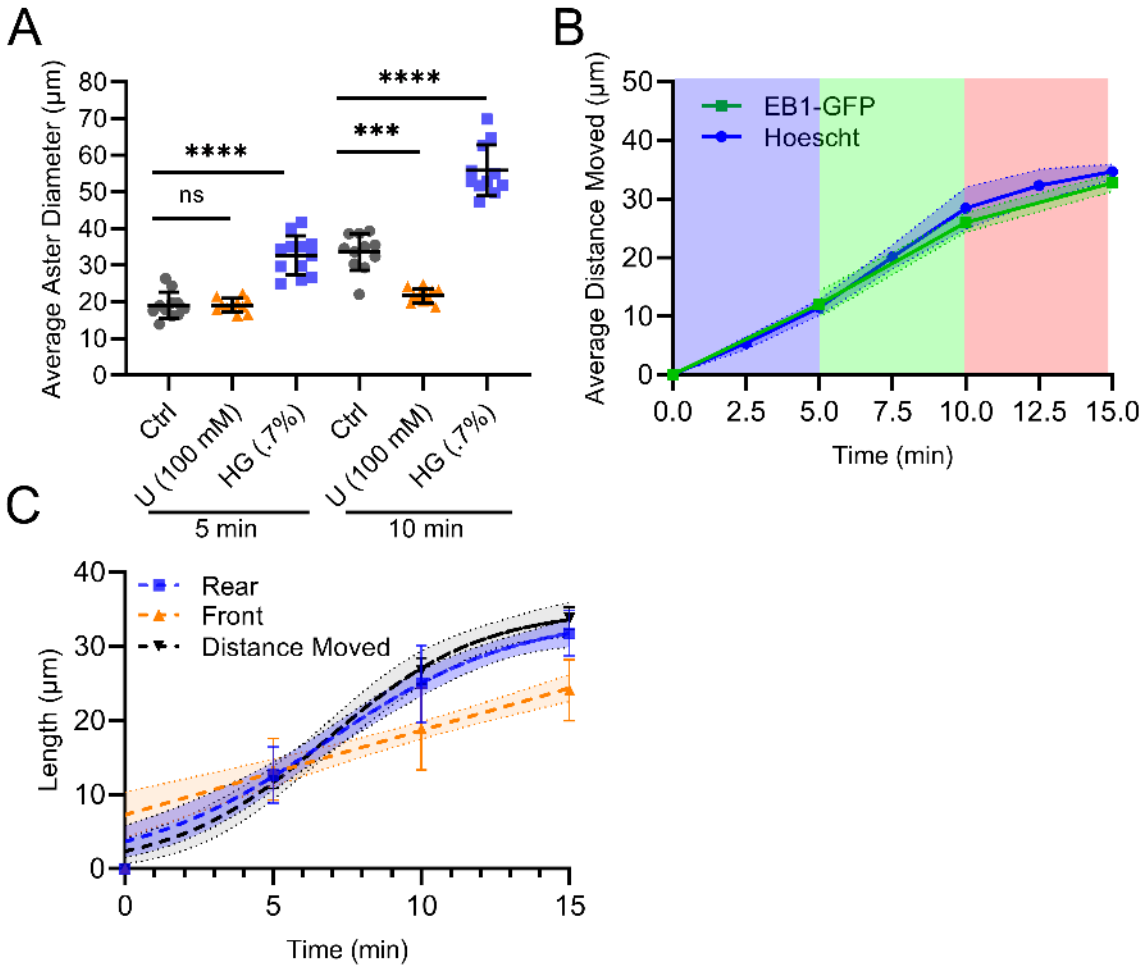

Figure S2. Additional analysis of aster diameters, migration dynamics, and comparison of migration dynamics with aster lengths, Related to Figure 2

(A) Aster diameters in different conditions quantified from z-stacks of fixed immunofluorescence images of zygotes represented by Figure 2A. ***P<.001, ****P<.0001 2-way ANOVA with Tukey's multiple comparisons test. Each shape is the diameter of an individual aster. Data are represented as the mean, ± SD (n=11 zygotes).

(B) Comparison of average distance moved over time in control zygotes tracked by either the MTOC (EB1-GFP) or the male pronucleus (Hoescht labelling). Solid lines represent the mean, shaded areas ± SD (n=13 zygotes per condition). Each shaded area represents a region with a different slope/migration speed (2.29 +/-.09 µm, 4.8 +/- 2 µm, and 1.250 +/- .25 µm for blue, green, and red regions respectively). Statistical difference of the slopes was determined by a ANCOVA, P<.0001

(C) Comparison of aster migration rates with aster geometry. Shapes represent the mean Lfront, Lrear, and distance moved for n=12 zygotes (Orange, blue, and black shapes, respectively). Dotted lines correspond to the best fit logistic regression curves for each parameter. Distance moved and Lrear, R^2 of .803 and .984, respectively (P<.001). Lfront, R^2 of P=.84 (ns). Shaded areas represent 95% confidence interval.

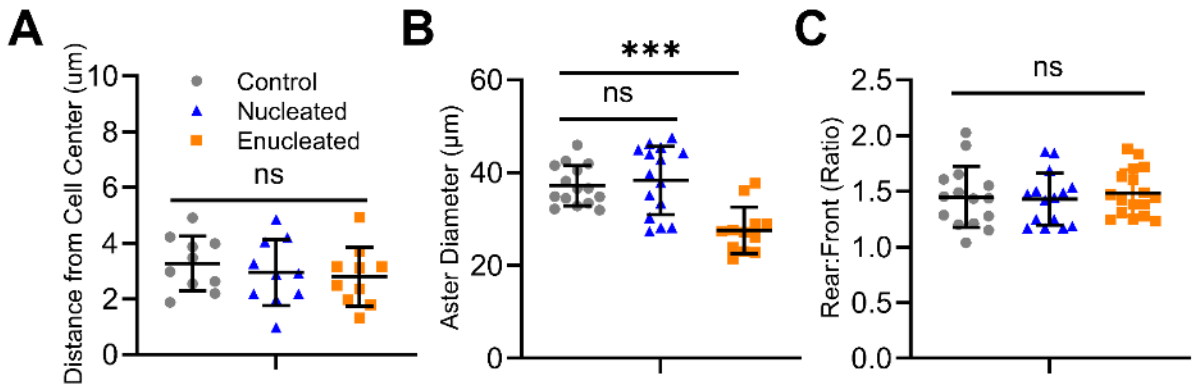

Figure S3. Characterization of Centration and Aster Geometry in Centrifuged enucleated and nucleated zygotes, Related to Figure 3

(A) Quantification of male pronuclear distance from the center of the zygote based on live-cell imaging of the male pronucleus (See Movie S3). The distance is not significantly different between non-centrifuged controls (gray circles), full-sized/nucleated centrifuged eggs (blue triangles), and enucleated centrifuged egg-halves (orange squares). One-way ANOVA, p>.5. Error bars represent SD (n=10 zygotes per condition)

(B) Average aster diameter of asters using the same conditions as in **(A)** based on immunofluorescence maximum intensity projections of sperm asters ~ 10 minutes post-sperm addition (See Figure 3D). Note aster diameter from non-centrifuged and full-sized/nucleated centrifuged eggs are not significantly different (p=.856, One-way ANOVA), while asters from smaller enucleated halves are significantly smaller (*** p>.0001, One-way ANOVA). Error bars represent SD (n=15 zygotes per condition). See STAR Methods for diameter measurement methods.

(C) Rear:Front aspect ratio of sperm asters using the same conditions as in **(A)** and **(B)** based on immunofluorescence maximum intensity projections of sperm asters ~10 minutes post-sperm addition. For all three conditions the Rear:Front aspect ratio is ~1.5, indicating that aster shape with regards to front and rear portions are not altered by centrifugation and enucleation. One-way ANOVA, p>.8. Error bars represent SD (n=15 zygotes per condition). See Star Methods for aspect ratio quantification methods.

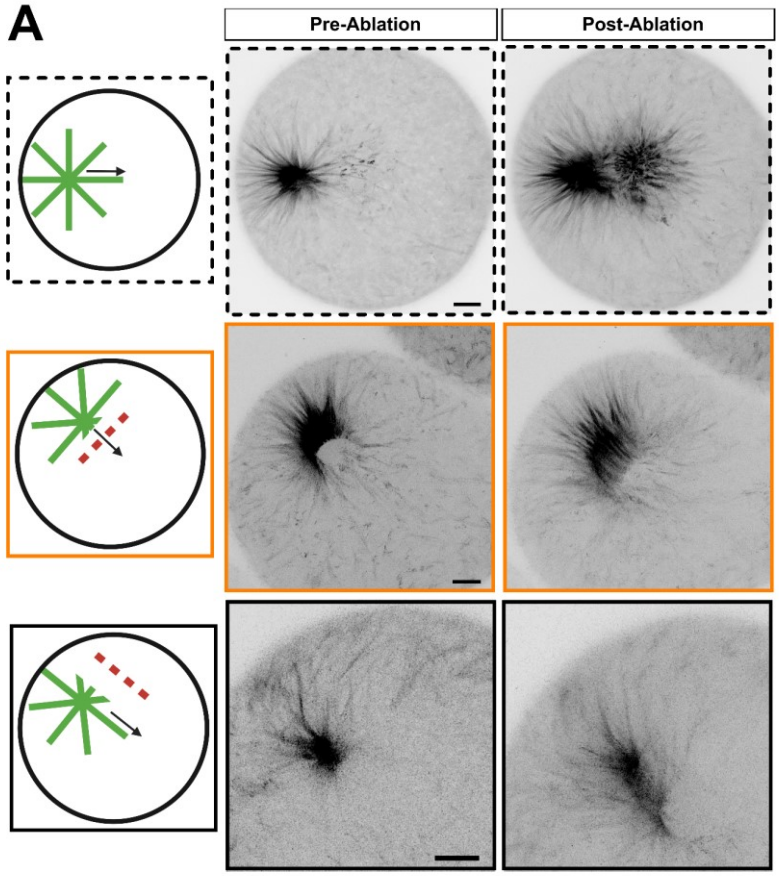

Figure S4. Front, side, and non-ablated sperm asters, Related to Figure 5

(A) Maximum temporal projections of non-ablated (top row), front-ablated (second row), and side ablated (bottom row) before and after activation of CA4 (Related to Figure 5B and 5C). The approximate regions of UV activation are indicated in the left illustrations. See also Movies S6 and S7. Scale bar,10 μm